Structure and faulting above a thick Messinian salt layer in the Levant basin (offshore Israel)

Estructura y fallamiento sobre una gruesa capa de sal messiniense en la cuenca de Levante (offshore de Israel)

Álvaro Carrión-Torrente[1], Juan Ignacio Soto[1,2], Moshe Reshef[3], Joan Flinch[4] and Ilson Nunes-Rubim[1]

[1] Departamento de Geodinámica, Universidad de Granada, Campus de Fuentenueva, 18071- Granada, España. alvct.91@gmail.com; inrubim@yahoo.com.br

[2] Instituto Andaluz de Ciencias de la Tierra (CSIC-Univ. Granada), 18071 - Granada, España. jsoto@ugr.es

[3] Department of Geosciences, Tel Aviv University, 69978 - Tel Aviv, Israel. moshe@luna.tau.ac.il

[4] Repsol Exploracion S. A., C/ Méndez Álvaro, 44, 28045-Madrid, España. jfflinch@repsol.com

ABSTRACT

The structure and deformation history of the supra-salt succession in a sector of the Levant Basin (offshore Israel) in the Eastern Mediterranean have been analysed. Through the interpretation of seismic cube migrated in depth, the main seismic discontinuities have been established in the Plio-Quaternary sequence, as well as the top and base of a thick salt layer of Messinian age (~1 km of thickness). A detailed seismic-stratigraphy has let to analyse the distribution of the supra-salt normal faults, as well as the pulses of syn-sedimentary faulting. At the same time as a ductile flow of the salt towards the NW, the cover was deformed and sank by means of SW-NE trending syn-sedimentary faults. During this deformation three main faulting pulses have been reconstructed (≤3.7, ~3.7-2.6, and ≤0.9 Ma).

Key-words: *salt tectonics, growth faulting, seismic interpretation, Messinian, Levant Basin.*

RESUMEN

Se analiza la estructura e historia de deformación en la sucesión supra-salina en un sector de la Cuenca de Levante (Israel) en el Mediterráneo Oriental. A través de la interpretación de un cubo sísmico migrado en profundidad se han establecido las principales discontinuidades sísmicas en la sucesión plio-cuaternaria, así como las reflexiones de techo y base de una potente lámina de sal de edad Messiniense (~1 km de espesor). Con una seísmo-estratigrafía detallada se han analizado la distribución de las fallas normales supra-sal, así como los pulsos de fallamiento sin-sedimentario. A la par que un flujo dúctil hacia el NO de la sal, la cobertera se deforma y hunde mediante fallas sin-sedimentarias SO-NE. En esta deformación se han reconstruido tres pulsos principales de fallamiento (≤3,7; ~3,7-2,6 y ≤0,9 Ma).

Palabras clave: *tectónica salina, fallas sin-sedimentarias, interpretación sísmica, Messiniense, Cuenca de Levante.*

Introduction

One of the main interests in salt tectonics comes from the oil industry, mainly because a large part of the world's hydrocarbon reserves is associated with evaporitic deposits (*e.g.*, Hudec and Jackson, 2011).

During the last years, large hydrocarbon discoveries have been found in the E Mediterranean basins (EMED) in relation to a thick Messinian salt deposit (Tamar, Leviathan, and Aphrodite discoveries; *e.g.*, Al-Balushi *et al.*, 2016). Salt tectonics processes in this basin are governed by a complex combination of gravity gliding and spreading (*e.g.*, Rowan *et al.*, 2012). These processes accommodate the downslope flow of the salt layer since at least the Messinian, accompanying the sedimentation of some of the salt sequences.

This work aims to analyse and characterise the structure of a deformed thick salt layer and its supra-salt sequence. In addition, the general shape and thickness of the salt body, and of the supra-salt faults will be studied through the detailed seismic interpretation of a depth-migrated seismic cube (PSDM; Feng and Reshef, 2016).

Geological setting

The seismic volume used in this work is located inside the Levant basin (LB). The LB is one of the EMED basins, and is located in the easternmost Mediterranean Sea, offshore Israel and Lebanon (Fig. 1). This basin is geologically delimited northward by the Cyprus Trench, southward by the Nile Cone, and by the Dead Sea Transform Fault in the east (Fig. 1).

The sedimentary sequence of the LB is formed mainly by marine carbonates, detritic and evaporitic materials, whose deposition started in the Mid-Permian and continues up to Present. The total sedimentary thickness in the basin has a maximum close to 15 km (Cartwright *et al.*, 2012).

The EMED are characterized by a thick sequence of evaporites deposited during the Messinian Salinity Crisis (MSC). This unit has been drilled, confirming that it is a layered sequence composed mainly by halite

with various highly reflective intra-salt levels (*e.g.*, Cartwright *et al.*, 2012; Feng *et al.*, 2016; Fig. 2).

Dataset

The seismic cube used in this study is a pre-stack depth migration volume (PSDM), migrated in depth using a three-dimensional velocity model constrained by well information. Feng and Reshef (2016) provide a detailed explanation of the velocity model and about the depth migration procedure. The seismic cube area is about 525 km^2 (~23 x 23 km) and the maximum penetration was 10 km. Seismic information below 3.2 km and the detailed position of the cube are not shown due to confidentiality.

A detailed 3D seismic interpretation of the boundaries (top and bottom) of the Messinian layer has been accomplished, together with a study of the deformations affecting the Plio-Quaternary, supra-salt sequence (Fig. 2).

Seismo-stratigraphy

The studied sedimentary sequence is separated in two main sequences: the Messinian salt and the supra-salt sequence (Fig. 2).

Based on the seismic character and continuity, the Messinian Salt Sequence has been divided in three evaporitic units with transparent seismic facies (ME1 to ME 3; Fig. 2A). These intra-salt sequences are bounded by high-amplitude reflective layers (MC1 to MC3; Fig. 2A). This seismo-stratigraphy follows the scheme used by many other authors in the LB (*e.g.*, Cartwright *et al.*, 2012).

ME1: The lowermost Messinian evaporite sequence, limited at the base by a high, negative amplitude reflection (BS), and bounded at the top by the MC1 reflective layer.

MC1: A relatively continuous flat reflection, bounding the ME1 and ME2 evaporitic sequences. MC1 is approximately parallel to BS, dipping northwestwardly. Feng *et al.* (2016) has demonstrated that MC1 is a fine-grained clastic layer.

ME2: This evaporitic sequence is a tabular unit with a rather constant thickness of 300 m.

MC2: This reflective package is composed by three (locally four) strongly deformed reflective layers, which are deformed by open folds and some low-angle thrusts.

ME3: This corresponds to the uppermost evaporitic sequence, which has some weak internal reflections onlapping with MC2. The upper part usually shows toplap geometries (towards the NW) with the top-salt (TS) contact.

MC3: In the northwest, above ME3, it appears a discontinuous level of high, positive amplitude reflections, which are truncated by TS. This level thickens northwestward.

The Plio-Pleistocene supra-salt sequence has been divided into four seismo-stratigraphic units (S1 to S4; Fig. 2A). The age of these sequences has been estimated by extrapolating linearly the age of the TS (5.3 Ma) to the seafloor:

S1 (Early Pliocene; Zanclean): The lower supra-salt unit is bounded by the TS and a seismic reflection estimated at ~3.7 Ma (Fig. 2A). This unit shows a sheet-like geometry and is characterized by moderate amplitude, highly continuous reflections, which are parallel to the TS. S1 has a mean thickness of 320 m that remain constant along the section. S1 is interpreted as hemipelagic deposits.

S2 (Late Pliocene; Piacenzian): The upper boundary of this unit is a moderate-reflective reflection estimated at ~2.6 Ma. S2 is characterized by highly continuous reflections with, low-to-moderate amplitudes. The parallel fabric of S2 is usually truncated by the upper boundary. This unit shows a rather constant thickness of about 60 m. Towards the centre of the area, it has been interpreted the occurrence of a subunit (called S2b; Fig. 2B) with a chaotic seismic facies and scarce internal reflections with low-reflectivity. S2b has a wedge geometry, thickening towards the SE, where it achieves a maximum vertical thickness of ~200 m.

S3 (Early Pleistocene; Gelasian and Calabrian): It is bounded by two erosive surfaces (Fig. 2B). The upper boundary has an estimated age of ~0.9 Ma. The lower boundary is a rough surface truncating the laminated fabric of the underlying S2 unit, which eliminates towards the NW the S2b unit. This unit has a chaotic seismic fabric
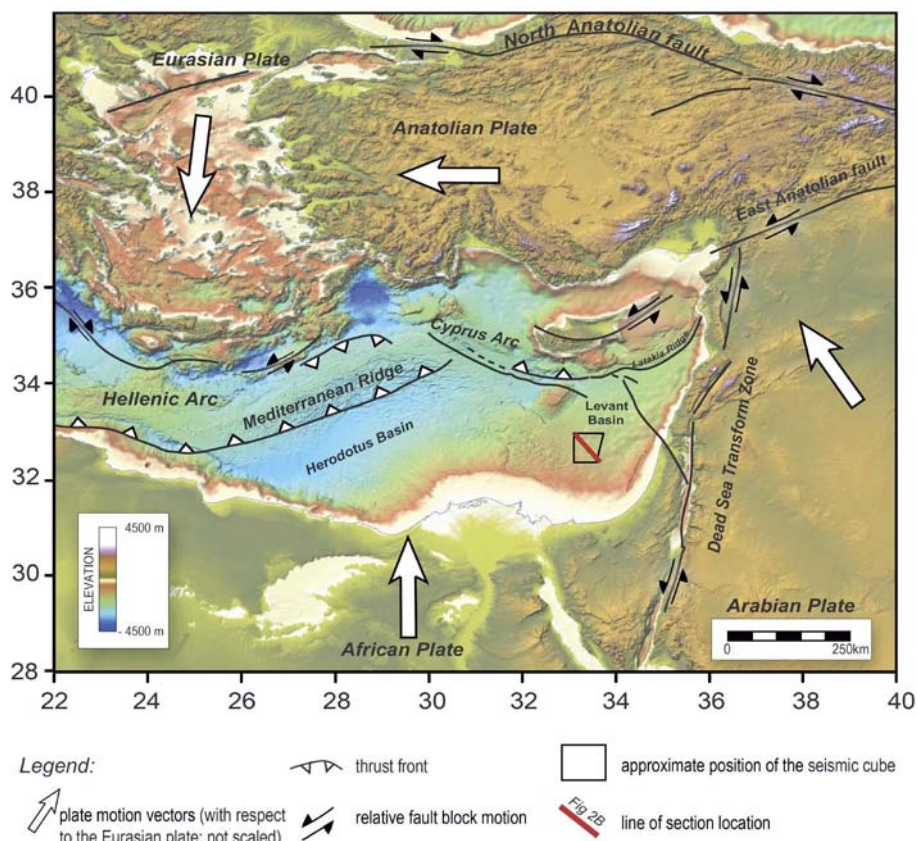

Fig. 1. - Tectonic map of the E Mediterranean Basins, locating the Levant Basin and the position of the studied seismic cube. Geology simplified from Allen *et al.* (2016). The position of Figure 2B is also shown. Ver figura en color en la web. See color figure in the web.

Fig. 1.- Mapa tectónico de las cuencas del este del Mediterráneo y localización de la cuenca de Levante y de la posición aproximada del cubo sísmico. Geología simplificada de Allen et al. *(2016). Se indica la posición de la figura 2B. Ver figura en color en la web.*
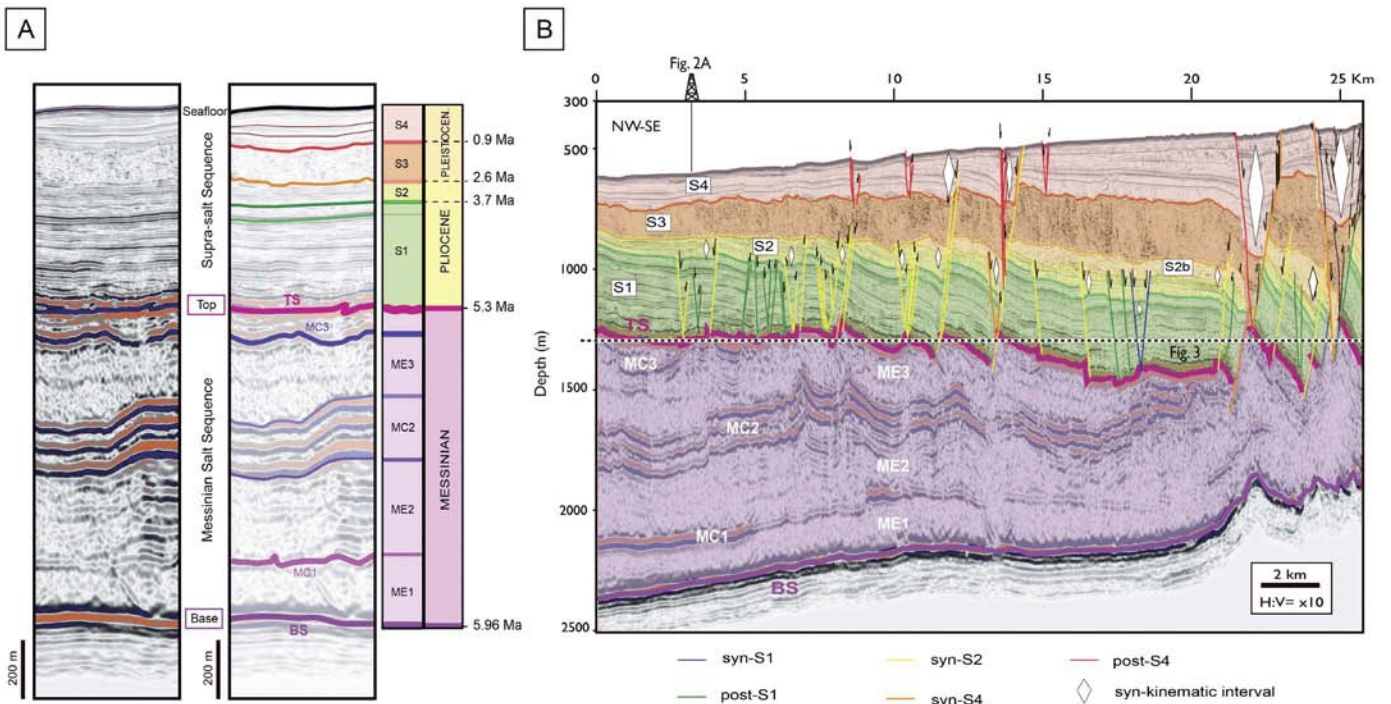
Fig. 2.- (A) Seismo-stratigraphy and acronyms used in the Levant Basin. The age of the seismic reflections has been calculated assuming a constant sedimentation rate extrapolated linearly from TS (5.3 Ma) to the seafloor. (B) Downdip NW-SE arbitrary seismic line and seismic interpretation focusing on the supra-salt extensional faults. Location of the section is shown in figure 1. See color figure in the web.

Fig. 2.- (A) Esquema sismo-estratigráfico y acrónimos usados en la Cuenca del Levante. La edad de los horizontes principales se ha calculado suponiendo una velocidad de sedimentación constante, extrapolada linealmente entre el techo de la sal (TS, 5,3 Ma) y el fondo marino. (B) Línea sísmica arbitraria NO-SE e interpretación centrándose en las fallas extensionales de la secuencia supra-sal. La localización de la sección se muestra en la figura 1. Ver figura en color en la web.

with moderate low-amplitude reflections, and has wedge geometry, thickening towards the SE (Fig. 2B). The thickness varies from 330 to 70 m. This unit possibly corresponds to a mass transport deposit.

S4 (since Middle Pleistocene): The base of this unit is an irregular, erosive surface (Fig. 2B). Internally, this unit has scarce, low-to-moderate amplitude reflections and shows wedge geometry, thickening towards the SE. With respect to the base, S4 shows downlap truncations. Maximum thickness is ~500 m thinning towards NW to up few tens of meters.

General structure

The general geometry of the region is illustrated in figure 2B. This is a downdip arbitrary seismic line oriented NW-SE. The Messinian salt body is broadly tabular along this selected profile. The unit thickening towards the NW, achieving a maximum thickness of ~1500 m, decreasing until being less than 400 m. Salt thickening is related to the ductile flow of the Messinian salt layer, migrating downslope towards the NW in the margin (Allen *et al.*, 2016).

The lower intra-salt unit, ME1, is concordant with BS and has a constant thickness of around 200 m. The middle-unit, ME2, is a tabular layer with an irregular top surface and achieves maximum thicknesses > 300 m in the internal salt anticline structures. Towards the LB margin (*i.e.*, towards the SE), the different evaporitic sequences (ME1 to ME3) cannot be distinguished, and a single, transparent layer constitutes the Messinian salt sequence (Fig. 2B). The uppermost evaporites in fact, thin abruptly towards the TS, coinciding with a major fault zone dipping basinward towards the NW. Internally, the Messinian sequence shows internal folds, like the open anticlines depicted by the reflective package MC2. In detail, most of these folds have NW vergence, *i.e.*, basinward (*c.f.*, between 5 and 10 km in Fig. 2B).

The overlying, Plio-Pleistocene supra-salt sequence thickens landward, achieving a maximum vertical thickness of 1 km, whereas it thin progressively towards the NW, up to a minimum of ~500-600 m. The supra-salt sequence is affected by planar normal faults.

The lower half of the Plio-Pleistocene succession (S1 and S2 units; *i.e.*, Pliocene)

is approximately tabular and it does not change significantly towards the faults. In contrast, the upper part of this succession (S2b, S3 and S4 units; *i.e.*, since the latest Piacenzian) thickens, towards and across the faults, defining a series of syn-sedimentary grabens opening landwards (Fig. 2B).

The top of the salt sequence is also affected by normal faults. The general trend of this surface is mainly sub-horizontal with local highs and lows, dipping gently towards the SE (Fig. 2B), where it achieves a maximum depth of 1400 m. Shallower depths (< 1200 m) are achieved towards the NW and above the crest defined by the fault zone at the SE (Fig. 3).

The base (BS) of the Messinian sequence is nearly flat and has a gently NW dip (<5º). Depth of the BS varies from about 2 km at the SE to 2.4 km towards the NW.

Supra-salt faulting

The supra-salt sequence is characterized by planar normal faults with small salt rollers and rollover folds.

These faults are planar fractures with a maximum displacement of 200 m in the

central domain of the section, increasing the fault displacement magnitude towards the SE (Fig. 2B).

The dips of the studied fault population vary along the section (Fig. 2B). The dominant family is formed by normal faults dipping 45°- 55° towards NW; other conjugate and contemporaneous faults dip toward SE, with higher dips of 55°- 60°.

Both faults families are linked, forming angles of 70°-80°. This geometry contrasts with the common dihedral angle (~60°) observed between conjugate faults during brittle faulting under compressional vertical stress, thus reflecting a non-Coulomb behaviour during faulting.

A clockwise rotation (i.e., towards the SE) of the initial position of the blocks together with the planar faults is found (Fig. 2B). This rotation increases towards the SE and it is shown by the lower dip of the master faults in relation to their relative conjugate, antithetic faults. This fault rotation is accomplished above a weak salt layer, which acts as an effective detachment surface during extension of the supra-salt sequence.

In plan view (Fig. 3), it is interpreted the occurrence of SW-NE extensional fault systems. These normal fault systems are formed by several normal fault segments, which dip northwestwards, and their conjugate faults, dipping opposite, describing a horst-graben system. The morphology of the fault planes is normally convex upward with the apex located in the vicinities of the
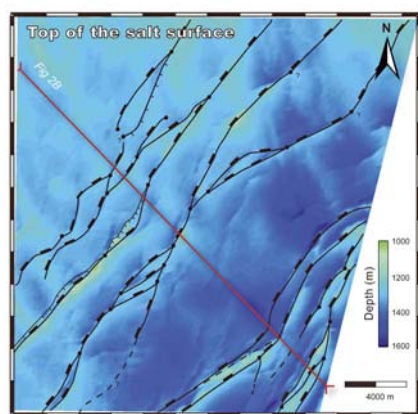

Fig. 3.- Structural depth map of the top of the Messinian salt sequence (TS). Included faults correspond to the structure interpreted at 1250 m depth (See position in Fig. 2B). See color figure in the web.

Fig. 3.- Mapa estructural de profundidad para el techo de la secuencia salina (TS). Incluye las fallas interpretadas a una profundidad de 1250m (ver posición en Fig. 2B). Ver figura en color en la web.

region with the maximum displacement. This geometry responds, possibly, to an upward bending of the fault surface produced by the salt upwelling during faulting.

The analysis of faults distribution with respect to the different seismic units allowed us to define various pulses of faulting. Most of the faults affect only the seismic units S1 and S2, whereas others cut all the Plio-Quaternary succession. There is a third set of small faults that only affects the upper seismic unit, S4 (Fig. 2B).

The timing of deformation varies also along the area. During the first faulting pulse, few normal faults were syn-sedimentary with the top of Unit S1 (3.7 Ma; Fig. 2B). Lately, during the second pulse, it started to develop another set of syn-sedimentary faults during the deposit of S2 (between ~3.7 and 2.6 Ma.) There was then a deformation pause coinciding with the sedimentation of S3 (~2.6-0.9 Ma). Afterwards, and during the third pulse, the youngest faults start their activity coinciding with the deposition of Unit S4 (≤ 0.9 Ma). During this stage some of the previous faults were also reactivated (Fig. 2B). The faulting mechanisms in the Levant basin are probably driven by a combination of gravity spreading triggered by the sediment load, and the downslope gliding of the Messinian evaporite sequence.

Conclusions

The main conclusions obtained in this work are:

(1) The Messinian salt body in the Levant basin defines a NW-thickening wedge of salt, which achieves up to 1.5 km of vertical thickness. A flat base and a strongly deformed top bound this salt layer. Within this evaporite sequence, we have found various transparent layers formed mainly by halite (ME1-ME3) separated by three reflective layers mostly composed by shales (MC1-MC3).

(2) The Plio-Quaternary sequence is characterised by 4 seismic units, locally 5 (S1-S2-S2b-S3-S4) and achieves ~1 km of vertical thickness. These materials describe a wedge, which thickens landward (*i.e.,* SE).

(3) The supra-salt sequence is deformed by SW-NE trending normal faults (mainly dipping towards NW), forming conjugate fault systems. The morphology of the fault planes is sometimes convex upwards, due

possibly to fault up warping induced by the salt upwelling during faulting.

(4) The timing of normal faulting varies along the studied area. After the deposit of unit S1, three main pulses of faulting occurred. The first episode occurred during the late lower Pliocene (≤3.7 Ma), coinciding with the deposition of the upper S1. A second pulse accompanied the sedimentation of S2 (Late Pliocene; ~2.6 Ma) and a third, during deposition of S4 in the middle Pleistocene (≤ 0.9 Ma). These faulting pulses were probably driven by a combination of gravity downslope (basinward; *i.e.*, NW) gliding and spreading of the thick Messinian salt layer in the Levant Basin.

Acknowledgements

Referencias

Al-Balushi, A., Fraser, A.J., Jackson, C.A.-L. and Allen, P.A. (2016). *Petroleum Geoscience* 22, 357-379.

Allen, H., Jackson, C.A-L. and Fraser, A.J. (2016). *Petroleum Geoscience* 22, 340-356.

Cartwright, J., Jackson, M., Dooley, T. and Higgins, S. (2012). In: *Salt Tectonics, Sediments and Prospectivity* (Alsop, G.I., Archer, S.G., H., Grant, N.T. and Artley, A.J. Hodgkinson, R., Eds.). Geological Society, London, Special Publications 363, 449-470.

Feng, Y.E. and Reshef, M. (2016). *Petroleum Geoscience* 22, 333-339.

Feng, Y.E., Yankelzon, A., Stainberg, J. and Reshef, M. (2016). *Marine Geology* 376, 118–131.

Hudec, M.R. and Jackson, M.P.A. (2011). The salt mine: a digital atlas of salt tectonics. *AAPG Memoir* 99, 324 p.

Rowan, M.G., Peel, F.J., Vendeville, B.C., and Gaullier, V. (2012). *Marine and Petroleum Geology* 37, 184-194.